

## Supplementary Materials for

### **Proliferation of cells with HIV integrated into cancer genes contributes to persistent infection**

Thor A. Wagner, Sherry McLaughlin, Kavita Garg, Charles Y. K. Cheung,  
Brendan B. Larsen, Sheila Styrchak, Hannah C. Huang, Paul T. Edlefsen,  
James I. Mullins, Lisa M. Frenkel\*

\*Corresponding author. E-mail: lfrenkel@uw.edu

Published 10 July 2014 on *Science* Express  
DOI: 10.1126/science.1256304

#### **This PDF file includes:**

Materials and Methods  
Figs. S1 to S3  
Tables S1 and S2  
References

**Other Supplementary Material for this manuscript includes the following:**  
(available at [www.sciencemag.org/cgi/content/full/science.1256304/DC1](http://www.sciencemag.org/cgi/content/full/science.1256304/DC1))

Table S3 (as Excel file)

## MATERIALS and METHODS

**Study population.** HIV-1 infected individuals were enrolled prior to initiation of ART, and had study blood collected at regular clinic visits, in accordance with a protocol approved by the Seattle Children's Institutional Review Board for Human Subjects. Clinical parameters, including plasma HIV RNA, CD4 cell counts and prescribed antiretroviral drugs were extracted from participants' medical records. Children with median plasma HIV-1 RNA levels of <50 copies/mL for >10 years of ART with available banked specimens were selected for this study (2, 8, 44).

**HIV integration site loop amplification (ISLA) assay.** The ISLA assay is outlined in Figure S1. To develop and optimize the method, DNA extracted from ACH-2 cells, a T cell clone with one common integrated proviral copy (46, 47), was mixed with DNA from Molt-4, a HIV-uninfected lymphoblast clone (48, 49) at diminishing concentrations of ACH-2 DNA.

**Extraction and quantification of HIV DNA.** Nucleic acids were extracted from cell lines and HIV-infected participants' peripheral blood mononuclear cells (PBMC) using the Gentra DNA purification system (Qiagen, Valencia, CA) or the ArchivePure DNA purification system (5 Prime, Gaithersburg, MD). HIV DNA was quantified by nested PCR of *env* (C2V5 region) using serially diluted nucleic acids (three replicates of each 5-fold dilution) and the QUALITY software program (50); <http://indra.mullins.microbiol.washington.edu/quality/>.

**Linear extension reactions.** For unidirectional amplification of the proviral DNA from HIV *env* through the site of chromosomal integration two forward primers were used, one in HIV *env* and one in HIV *nef* (Figure S1, Step 1). These primers were combined with ~3 copies of proviral DNA, as quantitated above (3 copies were typically required to achieve 30% success in integration site amplification reactions). Multiple linear reactions were conducted with each specimen (~100 reactions to achieve 30 positive reactions). The DNA was combined with 15 pmol each of primers env.6880F (5'-CCCGGGCTGGTTTGCGATTCTAAAGTGTA-3') and

nef.8948F (5'-CCAATGCTGATTGTGCCTGGCTAGAAGCA-3'), and 1x Advantage2 buffer (Clontech, Palo Alto, CA), 200 uM dNTPs, 5 U NotI (New England Biolabs, Ipswich, MA), and 0.5uL of Advantage2 50x polymerase in 50 uL total reaction volumes. The reactions were incubated as follows: 30 minutes (min) at 37°C, 2 min at 95°C, followed by 30 cycles of 20 seconds (sec) at 94°C, 30 sec at 60°C and 3 min at 72°C.

Bind random decamers tailed with a U5-specific primer sequence. To create a reverse primer site for loop formation of the proviral integration site and adjacent human sequence, random decamers tailed with a U5-specific primer (deca1.U5; 5'-TCAAGTAGTGTGTGCCCGTCTGTNNNNNNNNNN-3') were hybridized to an aliquot of the single-stranded linear extension reaction generated in Step 1 ([Figure S1, Step 2](#)). This primer was extended by combining 13 uL of the linear extension reaction with 40 pmol of deca1.U5 and 2.5 U of MyTaq in 0.5x MyTaq buffer (Bioline, London, UK) in a total volume of 20 uL. Concurrently, to stabilize the unused single-stranded template during storage, the remaining ~37uL of each linear-extension reaction was converted to double-stranded DNA by adding 15 pmol of deca1.U5 primer and 2.5 U of MyTaq in a total volume of 50 uL.

Both sets of reactions were incubated at 68°C for 2 min, cooled to 65°C for 1 min, and then progressively cooled by 1°C per minute until reaching 25°C. The reactions were reheated to 60°C and ramped down by 1°C per minute, as before, until reaching 20°C. Following the two ramped cooling steps, the 50uL reactions were stored at -20°C.

Trim ends of duplex fragments. Using the 20uL reactions from Step 2, the single-stranded DNA 3' to the random decamer annealing site was removed by addition of 10 U of Exonuclease 1 (Exo1) (New England Biolabs, Ipswich, MA), followed by incubation at 37°C for 45 min ([Figure S1, Step 3a](#)). To ensure complete digestion by Exo1, the temperature was then increased by 1°C, at intervals of 3 minutes, until reaching 43°C to melt any template partially annealed to the

U5 region of the primer. The reactions were then incubated at 72°C for 15 min to allow extension by MyTaq of the region complementary to the U5 primer sequence ([Figure S1, Step 3b](#)), followed by 5 min at 95°C to inactivate Exo1.

Form and extend loops and 1<sup>st</sup>-round PCR amplification. The fragments from Step 3 were subsequently cycled through denaturing/annealing/extension steps in the presence of MyTaq and the 1<sup>st</sup>-round PCR primer (RF2). Because the 3'-end of the fragment was engineered to bind to its complementary site in U5, hybridization will result in the formation of a loop ([Figure S1, Step 4a](#)). MyTaq will extend from the U5 priming site, through the end of the fragment, creating a loop of human genomic sequence with the HIV LTR duplicated on each end ([Figure S1, Step 4b](#)). Once the loop is formed and the LTR is duplicated, the RF2 primer can bind and begin amplification ([Figure S1, Step 5](#)).

These looping/1<sup>st</sup>-round PCR reactions were composed of 20uL of the product from Step 3, 1x MyTaq buffer, 30 pmol RF2 primer (5'-TCTGAGCCTGGAGCTCTTG-3') and 3.75 U of MyTaq in a total volume of 50 uL. Reactions were incubated for 2 min at 95°C; followed by 10 cycles of 20 sec at 94°C, 30 sec at 60°C, and 2 min at 72°C; then followed by 40 cycles of 10 sec at 92°C, 15 sec at 65°C, and 2 min at 72°C; and a final 5 min incubation at 72°. Additional second and third round PCR reactions with nested LTR primers were performed to ensure a product that was specific, and could be visualized on a gel. Second round PCR mixtures contained 5 uL of the 1<sup>st</sup> round reaction, 30 pmol of RF1 (5'-TTAAGCCTCAATAAGCTTGCCTTG-3'), 1x MyTaq buffer and 3.75 U MyTaq in 50 uL. Third round PCR mixtures contained 2 uL of the 2<sup>nd</sup> round reaction, 30 pmol of 1.U5 (5'-TCAAGTAGTGTGTGCCCGTCTGT-3'), 1x MyTaq buffer and 3.75 U MyTaq in 50 uL. Cycling parameters were the same for both: 2 min at 95°C, followed by 34 cycles of 20 sec at 94°, 30 sec at 65° and 2 min at 72°, and a final 5 min incubation at 72°C.

Identify chromosomal integration site. Third round-PCR products from Step 5 were identified by gel electrophoresis and sequenced using 2.U5 (5'-GTTGTGTGACTCTGGTAAGTAGAGAT-3'), an U5-specific primer located downstream of the looping site. Sequences were edited using Sequencher v5.0.1 and the last 40 bases of the HIV 3' LTR sequence was used to pinpoint the site of provirus integration into the human genome ([Figure S1, Step 6](#)).

Design primers to integration sites. Nested primers were designed in the human sequence 3' to each integration site.  $T_m$ s ranged from 62° - 68°C (based on Integrated DNA Technologies' OligoAnalyzer; <https://www.idtdna.com/analyizer/Applications/OligoAnalyzer/>), and when possible, the  $\Delta G$  for the 3' end was less negative than -7.5 kcal/mol. If the integration happened to occur near or within a repetitive element, the primer was designed so that it did not overlap the element ([Figure S1, Step 7](#)). All primer sequences were analyzed using Primer-BLAST (51) to identify whether primers would likely amplify unintended regions of the human genome.(51) If necessary, the primers were revised to specifically amplify the intended target. Because each env amplification used a unique primer, there were no positive control DNA templates to optimize the PCR primers or conditions.

Amplification and sequencing of HIV env linked to integration sites. Forty-five uL of the saved linear extension reaction from Step 2 was combined with 90 pmol of env.6984F (5'-ACAGTACAATGTACACATGGAATTA-3'), 90 pmol of the outer integration site-specific primer, 200 nM dNTPs, 1x Advantage2 buffer and 0.5 uL Advantage2 50x polymerase in a total volume of 300 uL. This was split into three 100 uL aliquots and cycled as follows: 2 min at 95°, followed by 45 cycles of 10 sec at 94°C, 15 sec at 65°C, and 3 min at 68°C, and ending with 5 min at 72°C. The 2<sup>nd</sup>-round PCR contained 5 uL of 1<sup>st</sup>-round product, 15 pmol of env.6963F (5'-TGGAATTAGGCCAGTAGTATCAACTCA-3'), 15 pmol of the inner integration site-specific primer, 200 nM dNTPs, 1x Advantage2 buffer and 0.5 uL Advantage2 in a total volume of 50 uL ([Figure S1, Step 8](#)). Cycling parameters were the same as for 1<sup>st</sup>-round PCR, except the

number of cycles was decreased to 34. Positive reactions were detected by gel electrophoresis and the C2V5 region of HIV *env* was bi-directionally sequenced with the primers DR7 (52) and BH2 (53).

Laboratory procedures to reduce the risk of amplicon carryover contamination. We used a separate area within the laboratory to set-up 1<sup>st</sup>-round PCR without exposure to potentially contaminating PCR amplicons. Given that our method includes three rounds of PCR, a second area was designated solely to set-up 2<sup>nd</sup>-round PCR. The benchtop was covered with a disposable absorptive pad that was replaced frequently. Pipet tip boxes were assigned for exclusive use in this area and pipettors were wiped with soap and water prior to use.

Alignment of human sequences with integrated provirus. Bowtie 2 (54) was used to align all trimmed sequences against *human genome* version 19 (hg19). The top two alignments for each read that aligned at more than one location and whose alignment lengths were within one percent of each other were also aligned with BLAT (55). These alignments were mapped to known genes based on annotations from RefSeq genes (56) and UCSC known genes (57). For GO analysis and analysis involving comparison to known cancer genes, we only considered protein coding genes and characterized long non-coding RNAs. All integration sites were eventually mapped to a single chromosomal position.

**Gene Ontology (GO) Analyses:** Enrichment of GO terms for ontology biological process terms was tested with topGO package (58) in R using “classic” and “elim” methods and Fisher statistics. To identify GO terms enriched in genes with HIV integration compared to all human genes, we required the GO terms to be significant (*p*-value < 0.05) by both “elim” and “classic” methods. To define cancer-related GO categories, we used the 43 GO terms defined across 10 hallmarks of cancer (23, 24) from a recent study (25).

**Statistical Methods.** For comparison of two-by-two contingency tables, we applied two-sided Fisher's exact tests (58) at the standard 5% type-I error rate. For evaluation of GO category enrichment of genes with integration sites in the three participants as compared with all genes in the human genome, we used the method described above. For evaluation of integration site enrichment for gene annotation features, which includes 1) the 43 hallmark cancer-related GO terms, tested individually and collectively as the inclusion of any of the terms, and 2) inclusion of the gene in the set of 1332 known cancer-related genes (11-15), we compared the fraction of (unique) integration sites that have the evaluated feature in each participant (pooled over the three time points) and in any participant (pooled over participants and time points) in our data to integration sites in Jurkat cells reported by Wang et al. (20). Specifically, the Jurkat cells data was used to construct a null distribution, as estimated by repeatedly uniformly sampling integration sites (with replacement) using a one-sided test at a 2.5% nominal type-I error rate. Individual GO annotations evaluated in this manner were corrected using the Holm-Bonferroni method (59) across the evaluated 43 hallmark GO terms. We repeated this analysis using only the subset of integration sites found multiple times (and therefore confirmed to be proliferating), pooled over participants. We also used the unique integration site samples to evaluate the null hypothesis that the number of unique integration sites per gene (among genes having any integration sites) is what would be expected if the observed unique sites followed the distribution found in the Jurkat cell data, and to evaluate the number of genes having integration sites observed in more than one of the three subjects. To evaluate trends over time in the percentage of unique integration sites that fall in genes having a particular feature (such as being a known cancer gene), we applied the Cochran-Armitage test (45) at a 5% nominal type-I error rate. All hypothesis tests were conducted using the R statistical computing language except as noted above, and p-values for individual analyses were not corrected for multiple comparisons except as noted above.

To evaluate whether the number of genes found to have insertion sites in more than one of the three subjects is significantly more than what would be expected by chance, given the number of genes found to have any integration sites in each subject, we conducted a one-sided hypothesis test (at nominal type-I error rate alpha = 0.025). We compared the observed number, 12, to a null distribution estimated by repeatedly counting the number of genes with at least two integrations across three sets of genes selected randomly from all genes observed to have any integrations in the Wang et al. dataset, with each gene set of size equal to the total number of genes for which any integration site was found in the corresponding subject. We sampled genes (without replacement) with probabilities proportional to the number of integration sites per gene observed in the Jurkat cell dataset.

This project was conceived and funding obtained by LMF, JIM; the project was designed by TAW, SM, JIM, LMF; specimens were collected by LMF, TAW; data were generated by SM, HCH, SS; data were analyzed by TAW, SM, KG, CYKC, PTE, JIM, LMF; and the manuscript was written by TAW, SM, KG, CYKC, PTE, JIM, LMF.

### **Supplemental Figures**

**Figure S1.** Overview of HIV integration site by loop amplification (ISLA)

**Figure S2.** Phylogenetic relationships between HIV-1 *env* (C2V5 region) genes sampled from participant B1 through time. Phylogenograms generated and labeled as described in the legend of Figure 2. In cases where HIV C2V5 *env* sequences were generated from cells that shared a specific integration site, the *env* sequences (~625bp) were identical. In contrast, among proviruses integrated at different chromosomal sites, only 3 clusters of sequences shared identical C2V5 sequences. Two of these clusters were made up of pairs of two sequences each, and when the entire C2*env*-nef-3'LTR region (~2.8kb) was sequenced, these differed by 2 mismatches in one case and 39 mismatches plus 2 indels (insertion/deletion) in the second. The

third cluster consisted of 4 sequences, two identical in the *C2env-nef*-3'LTR region and integrated in the same position in the CCDC64 gene; whereas the other sequences differed from the identical pair by 36 bases plus one indel, and 3 mismatches, respectively.

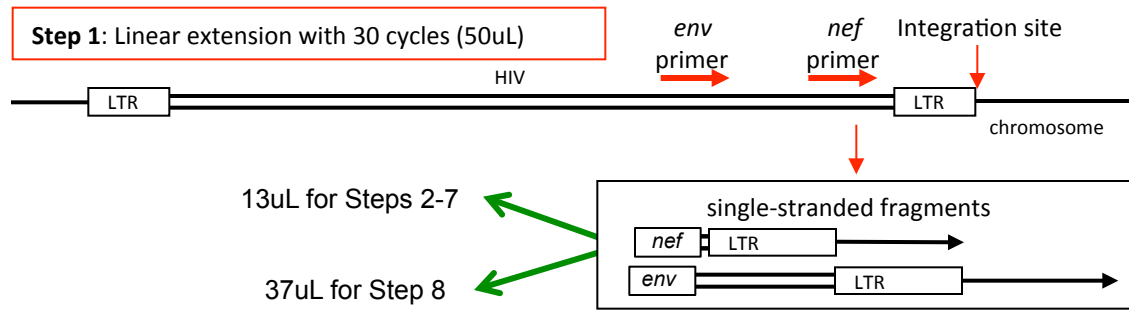
**Figure S3.** Phylogenetic relationships between HIV-1 env (C2V5 region) genes sampled from participant R1 through time. Sequences organized as described in the legend for Figure 2.

### Supplemental Tables

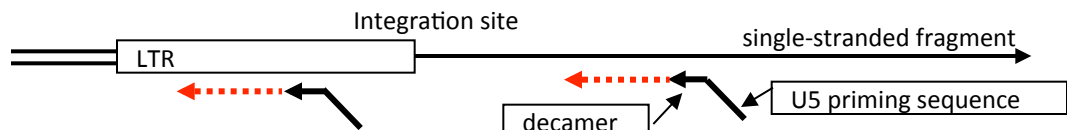
**Table S1. Panel A.** Genes with HIV integrations detected in multiple study participants, and detection of proliferating cells ( $\geq 2$  cells with identical integration site). **Panel B.** Genes with proliferating cells detected within each participant. **Panel C.** Multiple integration sites within the same gene found in a participant, without demonstrated proliferation.

**Table S2.** Top20 Gene Ontology (GO) terms overrepresented in ART-suppressed study participants compared to those annotated in the human genome.

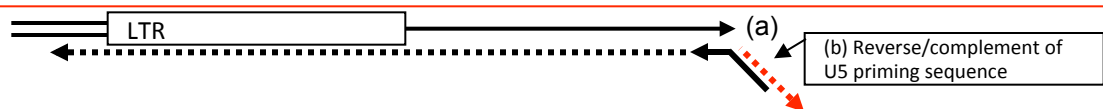
**Table S3.** Sequences of HIV-3'LTR and adjacent chromosome integration sites.



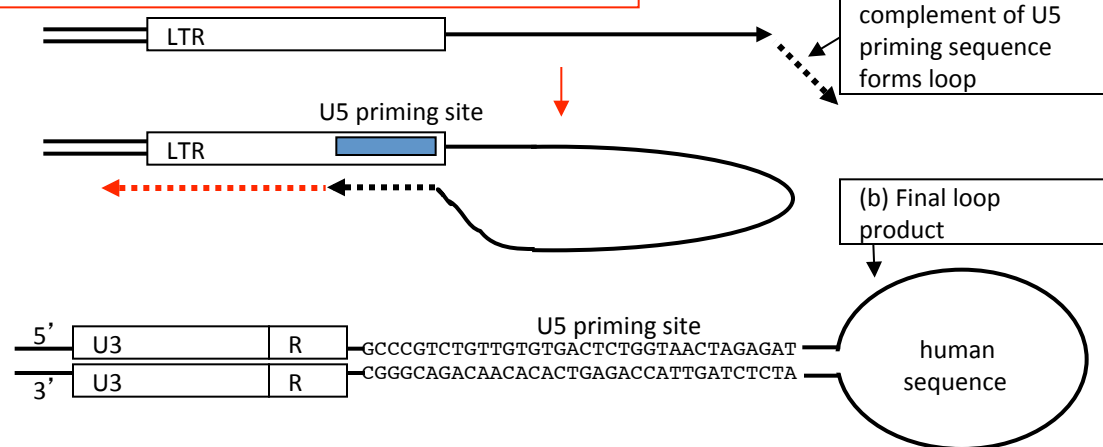
**Step 2: Bind random decamers tailed with a U5-specific primer sequence and extend**



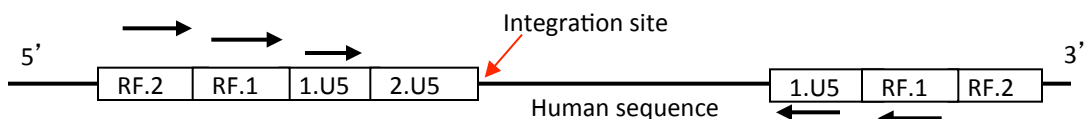
**Step 3: (a) Digest single-stranded fragment with Exo I; (b) Fill with Taq**



**Step 4: Denature, anneal to form loops and extend**



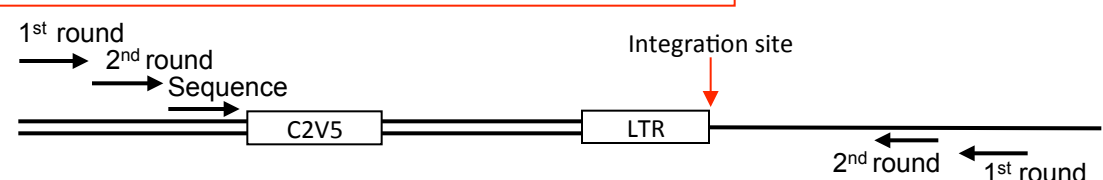
**Step 5: Amplify with nested R-region primers**

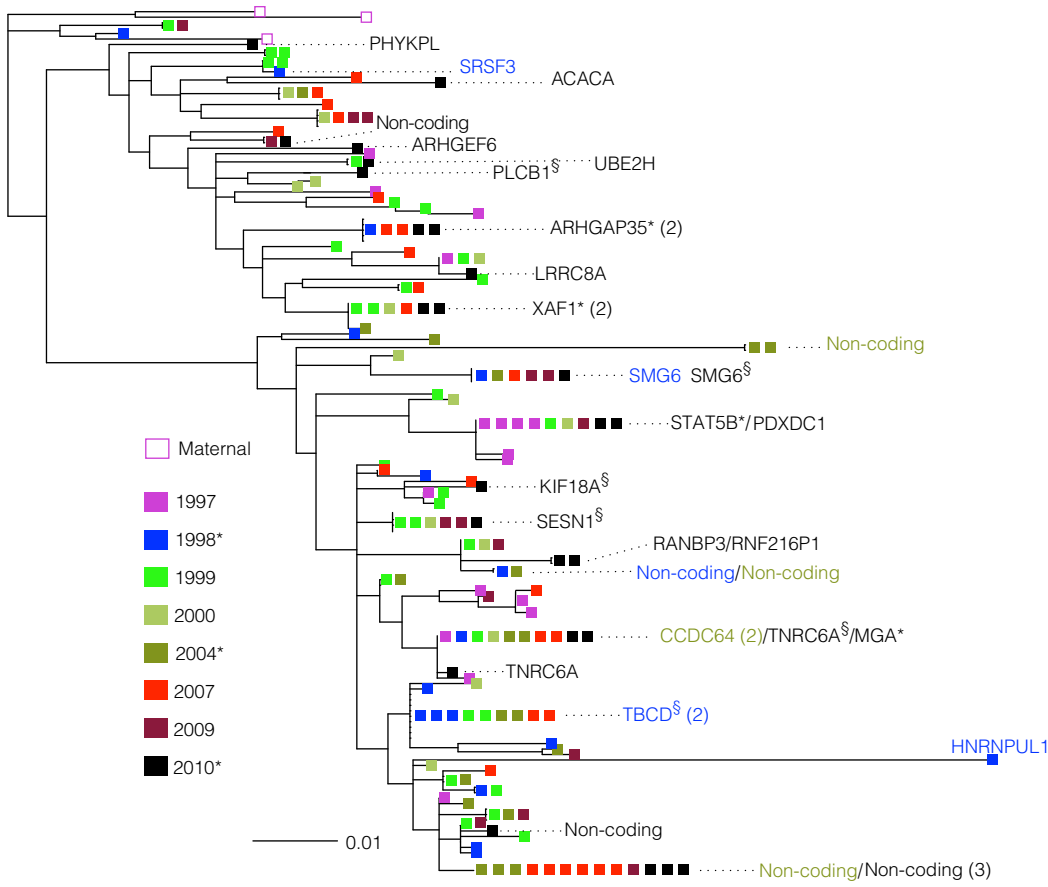


**Step 6: Sequence the integration site and identify the chromosome**

**Step 7: Design nested primers downstream of the integration site**

**Step 8: Amplify with nested env and chromosome primers**





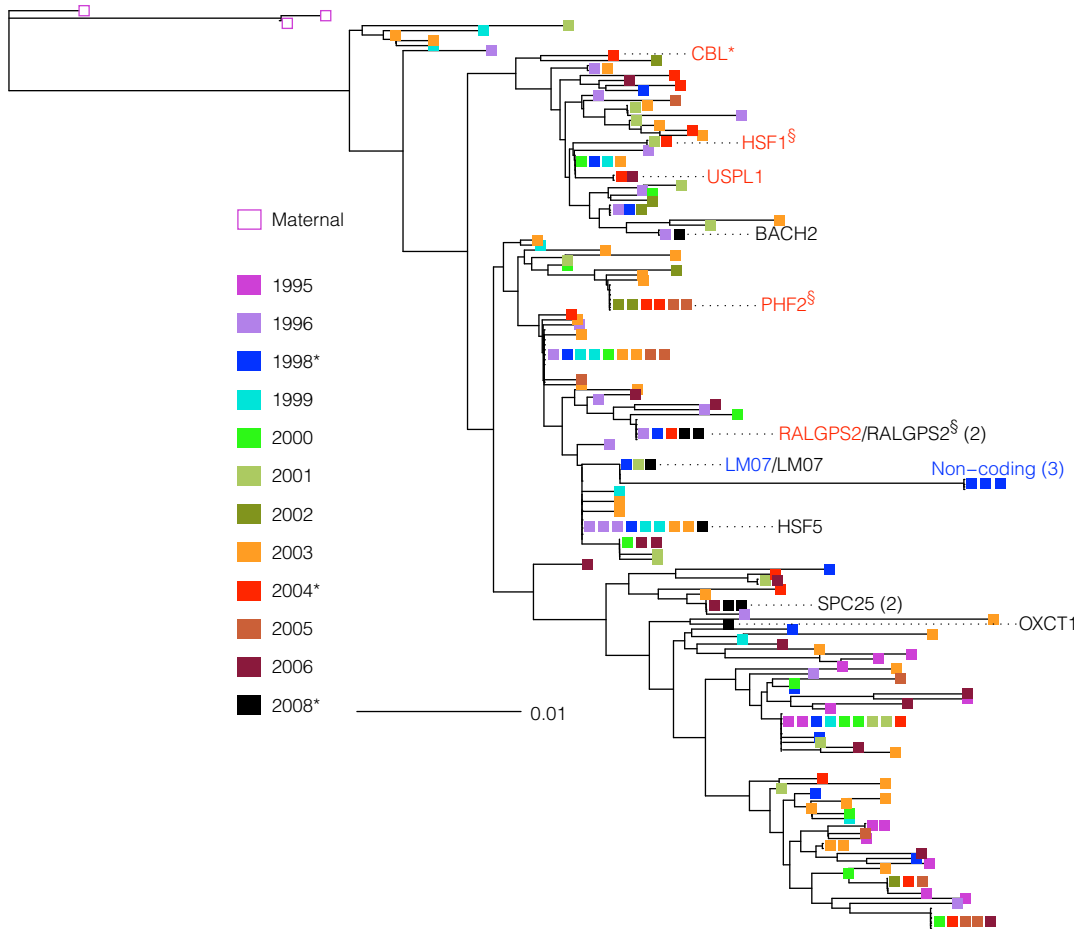


**Table S1, Panel A. Genes with HIV integrations detected in multiple study participants, and detection of proliferating cells ( $\geq 2$  cells with identical integration site)**

	Proliferation in 2 participants	Proliferation in 1 participant		No proliferation detected								
Gene:	BACH2	OXCT1	STAT5B*	ANKRD13C	C2CD3	CREBBP*	HNRNPUL1	IKZF3	KCTD13	MAPK1	ST8SIA4	TRAPPC10
<b>Participant-B1</b>												
# different integration sites			1			1	1		1	1		1
# times integration site detected			1			1	1		1	1		1
# same HIV C2V5 detected at other time points												
<i>Total # times detected in gene</i>			1			1	1		1	1		1
<b>Participant-L1</b>												
# different integration sites	7	1	3	1	1			1		1		1
# times integration site detected	4,2,1,1,1,1,1	1	1,1,1	1	1			1		1		1
# same HIV C2V5 detected at other time points												
<i>Total # times detected in gene</i>	11	1	3	1	1	1	1	1	1	1		1
<b>Participant-R1</b>												
# different integration sites	2	2		1	1	1	1	1	1	1		1
# times integration site detected	2,2	1,1		1	1	1	1	1	1	1		1
# same HIV C2V5 detected at other time points	1											
<i>Total # times detected in gene</i>	5	2		1	1	1	1	1	1	1		1

\* Indicates gene associated with cancer

**Table S1, Panel B. Genes with proliferating cells detected within each participant**

Gene:	ARHGAP35*	CCDC64	MOB1A*	MGA*	PDE3B	PRKCH	SESN	SMG6	SRSF3	TBCD	TNRC6A	UBE2H	WDR26	XAF1*
<b>Participant-B1</b>														
# different integration sites	1	1	1	1	1	1	1	2	1	1	1	1	1	1
# times integration site detected	2,2	4,1	2	1,2	2	2	1	1,9	2,1,1	5,1,1	1,2,2	1,2	3,2	3,3,3
# same HIV C2V5 detected at other time points	3						5	4		7				4
<i>Total # times detected in gene</i>	7	5	2	3	2	2	6	14	4	14	5	3	5	13

Gene:	ACSF3	APOBEC3C	GPC3*	MDC1	MKL2	RNF217
<b>Participant-L1</b>						
# different integration sites	1	1	1	1	3	1
# times integration site detected	3	1,1,2	2	7,16,9	2,1,1	2
# same HIV C2V5 detected at other time points	2	11		25		
<i>Total # times detected in gene</i>	5	15	2	57	4	2

Gene:	CBL*	HSF1	HSF5	LMO7	OXCT1	PHF2	RALGPS2	SPC25	USPL1	ZHX3
<b>Participant-R1</b>										
# different integration sites	1	1	2	1	1	1	1	1	1	1
# times integration site detected	2	2	1,1	1,1	1,1	5	1,4	4	2	3
# same HIV C2V5 detected at other time points		1	8	1		4	2	1	1	
<i>Total # times detected in gene</i>	2	3	10	3	2	9	7	5	3	3

\* Indicates gene associated with cancer

**Table S1, Panel C. Multiple integration sites within the same gene found in a participant, without demonstrated proliferation**

Participant/Gene:	B1	GCN1L1	NSMCE2	R1	GCN1L1	NSMCE2
# different integration sites		2	2		2	2
# times integration site detected		1,1	1,1		1,1	1,1
<i>Total # times detected in gene</i>		2	2		2	2

\* Indicates gene associated with cancer

**Table S2. Top-20 Gene Ontology (GO) terms overrepresented in ART-suppressed study participants compared to those annotated in the human genome**

GO Term^	Biological Function	Annotated Genes with given GO Term	Expected number of Genes	Genes with HIV integration	p value (elim)
GO:0000278*	mitotic cell cycle	824	13.38	31	0.00016
GO:0007173†	epidermal growth factor receptor signaling pathway	222	3.61	14	0.00019
GO:0051726†	regulation of cell cycle	725	11.77	25	0.00032
GO:0006491	N-glycan processing	9	0.15	3	0.00033
GO:0045944Ø	positive regulation of transcription from RNA polymerase II promoter	764	12.41	25	0.00069
GO:0019048Ø	virus-host interaction	364	5.91	15	0.00092
GO:0036092*	phosphatidylinositol-3-phosphate biosynthetic process	14	0.23	3	0.00135
GO:0006511	ubiquitin-dependent protein catabolic process	420	6.82	16	0.00143
GO:0048015*	phosphatidylinositol-mediated signaling	206	3.35	10	0.00202
GO:0032008*	positive regulation of TOR signaling	16	0.26	3	0.00203
GO:0033962	cytoplasmic mRNA processing body assembly	16	0.26	3	0.00203
GO:0009790	embryo development	980	15.92	30	0.00208
GO:0007219*	Notch signaling pathway	141	2.29	8	0.00214
GO:0043603†	cellular amide metabolic process	34	0.55	4	0.00215
GO:0045646	regulation of erythrocyte differentiation	34	0.55	4	0.00215
GO:0048011	neurotrophin TRK receptor signaling pathway	281	4.56	12	0.0022
GO:0022402†	cell cycle process	1074	17.44	37	0.00225
GO:0045070Ø	positive regulation of viral genome replication	17	0.28	3	0.00243
GO:0051294	establishment of spindle orientation	17	0.28	3	0.00243
GO:0061003	positive regulation of dendritic spine morphogenesis	5	0.08	2	0.00254

<sup>^</sup> The top 20 biologic functions enriched among the genes with HIV integration, ranked according to p-values generated by "elim" method and Fisher statistics

† Statistically significant ( $p < 0.025$ ) after controlling for multiple comparisons

\* Includes human cancer associated genes

ø Expected to have a strong influence on viral life cycle

## References

1. J. D. Siliciano, J. Kajdas, D. Finzi, T. C. Quinn, K. Chadwick, J. B. Margolick, C. Kovacs, S. J. Gange, R. F. Siliciano, Long-term follow-up studies confirm the stability of the latent reservoir for HIV-1 in resting CD4+ T cells. *Nat. Med.* **9**, 727–728 (2003). [Medline](#) [doi:10.1038/nm880](#)
2. N. H. Tobin, G. H. Learn, S. E. Holte, Y. Wang, A. J. Melvin, J. L. McKernan, D. M. Pawluk, K. M. Mohan, P. F. Lewis, J. I. Mullins, L. M. Frenkel, Evidence that low-level viremias during effective highly active antiretroviral therapy result from two processes: Expression of archival virus and replication of virus. *J. Virol.* **79**, 9625–9634 (2005). [Medline](#) [doi:10.1128/JVI.79.15.9625-9634.2005](#)
3. A. Sigal, J. T. Kim, A. B. Balazs, E. Dekel, A. Mayo, R. Milo, D. Baltimore, Cell-to-cell spread of HIV permits ongoing replication despite antiretroviral therapy. *Nature* **477**, 95–98 (2011). [Medline](#) [doi:10.1038/nature10347](#)
4. S. Letendre, J. Marquie-Beck, E. Capparelli, B. Best, D. Clifford, A. C. Collier, B. B. Gelman, J. C. McArthur, J. A. McCutchan, S. Morgello, D. Simpson, I. Grant, R. J. Ellis; CHARTER Group, Validation of the CNS Penetration-Effectiveness rank for quantifying antiretroviral penetration into the central nervous system. *Arch. Neurol.* **65**, 65–70 (2008). [Medline](#) [doi:10.1001/archneurol.2007.31](#)
5. C. V. Fletcher, K. Staskus, S. W. Wietgrefe, M. Rothenberger, C. Reilly, J. G. Chipman, G. J. Beilman, A. Khoruts, A. Thorkelson, T. E. Schmidt, J. Anderson, K. Perkey, M. Stevenson, A. S. Perelson, D. C. Douek, A. T. Haase, T. W. Schacker, Persistent HIV-1 replication is associated with lower antiretroviral drug concentrations in lymphatic tissues. *Proc. Natl. Acad. Sci. U.S.A.* **111**, 2307–2312 (2014). [Medline](#) [doi:10.1073/pnas.1318249111](#)
6. J. R. Bailey, A. R. Sedaghat, T. Kieffer, T. Brennan, P. K. Lee, M. Wind-Rotolo, C. M. Haggerty, A. R. Kamireddi, Y. Liu, J. Lee, D. Persaud, J. E. Gallant, J. Cofrancesco Jr., T. C. Quinn, C. O. Wilke, S. C. Ray, J. D. Siliciano, R. E. Nettles, R. F. Siliciano, Residual human immunodeficiency virus type 1 viremia in some patients on antiretroviral therapy is dominated by a small number of invariant clones rarely found in circulating CD4+ T cells. *J. Virol.* **80**, 6441–6457 (2006). [Medline](#) [doi:10.1128/JVI.00591-06](#)
7. N. Chomont, M. El-Far, P. Ancuta, L. Trautmann, F. A. Procopio, B. Yassine-Diab, G. Boucher, M. R. Boulassel, G. Ghattas, J. M. Brenchley, T. W. Schacker, B. J. Hill, D. C. Douek, J. P. Routy, E. K. Haddad, R. P. Sékaly, HIV reservoir size and persistence are driven by T cell survival and homeostatic proliferation. *Nat. Med.* **15**, 893–900 (2009). [Medline](#) [doi:10.1038/nm.1972](#)
8. T. A. Wagner, J. L. McKernan, N. H. Tobin, K. A. Tapia, J. I. Mullins, L. M. Frenkel, An increasing proportion of monotypic HIV-1 DNA sequences during antiretroviral treatment suggests proliferation of HIV-infected cells. *J. Virol.* **87**, 1770–1778 (2013). [Medline](#) [doi:10.1128/JVI.01985-12](#)
9. T. Ikeda, J. Shibata, K. Yoshimura, A. Koito, S. Matsushita, Recurrent HIV-1 integration at the BACH2 locus in resting CD4+ T cell populations during effective highly active antiretroviral therapy. *J. Infect. Dis.* **195**, 716–725 (2007). [Medline](#) [doi:10.1086/510915](#)

10. H. Imamichi, V. Natarajan, J. W. Adelsberger, C. A. Rehm, R. A. Lempicki, B. Das, A. Hazen, T. Imamichi, H. C. Lane, Lifespan of effector memory CD4+ T cells determined by replication-incompetent integrated HIV-1 provirus. *AIDS* **1** (2014). [Medline](#) [doi:10.1097/QAD.0000000000000223](https://doi.org/10.1097/QAD.0000000000000223)
11. S. A. Forbes, N. Bindal, S. Bamford, C. Cole, C. Y. Kok, D. Beare, M. Jia, R. Shepherd, K. Leung, A. Menzies, J. W. Teague, P. J. Campbell, M. R. Stratton, P. A. Futreal, COSMIC: Mining complete cancer genomes in the Catalogue of Somatic Mutations in Cancer. *Nucleic Acids Res.* **39** (Database), D945–D950 (2011). [Medline](#) [doi:10.1093/nar/gkq929](https://doi.org/10.1093/nar/gkq929)
12. M. S. Lawrence, P. Stojanov, C. H. Mermel, J. T. Robinson, L. A. Garraway, T. R. Golub, M. Meyerson, S. B. Gabriel, E. S. Lander, G. Getz, Discovery and saturation analysis of cancer genes across 21 tumour types. *Nature* **505**, 495–501 (2014). [Medline](#) [doi:10.1038/nature12912](https://doi.org/10.1038/nature12912)
13. M. Zhao, J. Sun, Z. Zhao, TSGene: A web resource for tumor suppressor genes. *Nucleic Acids Res.* **41** (D1), D970–D976 (2013). [Medline](#) [doi:10.1093/nar/gks937](https://doi.org/10.1093/nar/gks937)
14. C. Kandoth, M. D. McLellan, F. Vandin, K. Ye, B. Niu, C. Lu, M. Xie, Q. Zhang, J. F. McMichael, M. A. Wyczalkowski, M. D. Leiserson, C. A. Miller, J. S. Welch, M. J. Walter, M. C. Wendl, T. J. Ley, R. K. Wilson, B. J. Raphael, L. Ding, Mutational landscape and significance across 12 major cancer types. *Nature* **502**, 333–339 (2013). [Medline](#) [doi:10.1038/nature12634](https://doi.org/10.1038/nature12634)
15. B. Vogelstein, N. Papadopoulos, V. E. Velculescu, S. Zhou, L. A. Diaz Jr., K. W. Kinzler, Cancer genome landscapes. *Science* **339**, 1546–1558 (2013). [Medline](#) [doi:10.1126/science.1235122](https://doi.org/10.1126/science.1235122)
16. H. Fan, C. Johnson, Insertional oncogenesis by non-acute retroviruses: Implications for gene therapy. *Viruses* **3**, 398–422 (2011). [Medline](#) [doi:10.3390/v3040398](https://doi.org/10.3390/v3040398)
17. A. R. Schröder, P. Shinn, H. Chen, C. Berry, J. R. Ecker, F. Bushman, HIV-1 integration in the human genome favors active genes and local hotspots. *Cell* **110**, 521–529 (2002). [Medline](#) [doi:10.1016/S0092-8674\(02\)00864-4](https://doi.org/10.1016/S0092-8674(02)00864-4)
18. F. Bushman, M. Lewinski, A. Ciuffi, S. Barr, J. Leipzig, S. Hannenhalli, C. Hoffmann, Genome-wide analysis of retroviral DNA integration. *Nat. Rev. Microbiol.* **3**, 848–858 (2005). [Medline](#) [doi:10.1038/nrmicro1263](https://doi.org/10.1038/nrmicro1263)
19. R. S. Mitchell, B. F. Beitzel, A. R. Schroder, P. Shinn, H. Chen, C. C. Berry, J. R. Ecker, F. D. Bushman, Retroviral DNA integration: ASLV, HIV, and MLV show distinct target site preferences. *PLOS Biol.* **2**, e234 (2004). [Medline](#) [doi:10.1371/journal.pbio.0020234](https://doi.org/10.1371/journal.pbio.0020234)
20. M. J. Soto, A. Peña, F. G. Vallejo, A genomic and bioinformatics analysis of the integration of HIV in peripheral blood mononuclear cells. *AIDS Res. Hum. Retroviruses* **27**, 547–555 (2011). [Medline](#)
21. G. P. Wang, A. Ciuffi, J. Leipzig, C. C. Berry, F. D. Bushman, HIV integration site selection: Analysis by massively parallel pyrosequencing reveals association with epigenetic modifications. *Genome Res.* **17**, 1186–1194 (2007). [Medline](#) [doi:10.1101/gr.6286907](https://doi.org/10.1101/gr.6286907)

22. D. Persaud, G. K. Siberry, A. Ahonkhai, J. Kajdas, D. Monie, N. Hutton, D. C. Watson, T. C. Quinn, S. C. Ray, R. F. Siliciano, Continued production of drug-sensitive human immunodeficiency virus type 1 in children on combination antiretroviral therapy who have undetectable viral loads. *J. Virol.* **78**, 968–979 (2004). [Medline](#) [doi:10.1128/JVI.78.2.968-979.2004](#)
23. D. Hanahan, R. A. Weinberg, The hallmarks of cancer. *Cell* **100**, 57–70 (2000). [Medline](#) [doi:10.1016/S0092-8674\(00\)81683-9](#)
24. D. Hanahan, R. A. Weinberg, Hallmarks of cancer: The next generation. *Cell* **144**, 646–674 (2011). [Medline](#) [doi:10.1016/j.cell.2011.02.013](#)
25. C. L. Plaisier, M. Pan, N. S. Baliga, A miRNA-regulatory network explains how dysregulated miRNAs perturb oncogenic processes across diverse cancers. *Genome Res.* **22**, 2302–2314 (2012). [Medline](#) [doi:10.1101/gr.133991.111](#)
26. Y. Han, K. Lassen, D. Monie, A. R. Sedaghat, S. Shimoji, X. Liu, T. C. Pierson, J. B. Margolick, R. F. Siliciano, J. D. Siliciano, Resting CD4+ T cells from human immunodeficiency virus type 1 (HIV-1)-infected individuals carry integrated HIV-1 genomes within actively transcribed host genes. *J. Virol.* **78**, 6122–6133 (2004). [Medline](#) [doi:10.1128/JVI.78.12.6122-6133.2004](#)
27. Y. C. Ho, L. Shan, N. N. Hosmane, J. Wang, S. B. Laskey, D. I. Rosenbloom, J. Lai, J. N. Blankson, J. D. Siliciano, R. F. Siliciano, Replication-competent noninduced proviruses in the latent reservoir increase barrier to HIV-1 cure. *Cell* **155**, 540–551 (2013). [Medline](#) [doi:10.1016/j.cell.2013.09.020](#)
28. S. Swaminathan, C. Huang, H. Geng, Z. Chen, R. Harvey, H. Kang, C. Ng, B. Titz, C. Hurtz, M. F. Sadiyah, D. Nowak, G. B. Thoennissen, V. Rand, T. G. Graeber, H. P. Koeffler, W. L. Carroll, C. L. Willman, A. G. Hall, K. Igarashi, A. Melnick, M. Müschen, BACH2 mediates negative selection and p53-dependent tumor suppression at the pre-B cell receptor checkpoint. *Nat. Med.* **19**, 1014–1022 (2013). [Medline](#) [doi:10.1038/nm.3247](#)
29. R. Roychoudhuri, K. Hirahara, K. Mousavi, D. Clever, C. A. Klebanoff, M. Bonelli, G. Sciumè, H. Zare, G. Vahedi, B. Dema, Z. Yu, H. Liu, H. Takahashi, M. Rao, P. Muranski, J. G. Crompton, G. Punkosdy, D. Bedognetti, E. Wang, V. Hoffmann, J. Rivera, F. M. Marincola, A. Nakamura, V. Sartorelli, Y. Kanno, L. Gattinoni, A. Muto, K. Igarashi, J. J. O’Shea, N. P. Restifo, BACH2 represses effector programs to stabilize T<sub>reg</sub>-mediated immune homeostasis. *Nature* **498**, 506–510 (2013). [Medline](#) [doi:10.1038/nature12199](#)
30. S. Tsukumo, M. Unno, A. Muto, A. Takeuchi, K. Kometani, T. Kurosaki, K. Igarashi, T. Saito, Bach2 maintains T cells in a naive state by suppressing effector memory-related genes. *Proc. Natl. Acad. Sci. U.S.A.* **110**, 10735–10740 (2013). [Medline](#) [doi:10.1073/pnas.1306691110](#)
31. M. Kuwahara, J. Suzuki, S. Tofukuji, T. Yamada, M. Kanoh, A. Matsumoto, S. Maruyama, K. Kometani, T. Kurosaki, O. Ohara, T. Nakayama, M. Yamashita, The Menin-Bach2 axis is critical for regulating CD4 T-cell senescence and cytokine homeostasis. *Nat. Commun.* **5**, 3555 (2014). 10.1038/ncomms4555 [Medline](#) [doi:10.1038/ncomms4555](#)

32. J. Liu, A. B. Sørensen, B. Wang, M. Wabl, A. L. Nielsen, F. S. Pedersen, Identification of novel Bach2 transcripts and protein isoforms through tagging analysis of retroviral integrations in B-cell lymphomas. *BMC Mol. Biol.* **10**, 2 (2009). 10.1186/1471-2199-10-2  
[Medline doi:10.1186/1471-2199-10-2](#)
33. Y. Han, M. Wind-Rotolo, H. C. Yang, J. D. Siliciano, R. F. Siliciano, Experimental approaches to the study of HIV-1 latency. *Nat. Rev. Microbiol.* **5**, 95–106 (2007).  
[Medline doi:10.1038/nrmicro1580](#)
34. M. K. Lewinski, D. Bisgrove, P. Shinn, H. Chen, C. Hoffmann, S. Hannenhalli, E. Verdin, C. C. Berry, J. R. Ecker, F. D. Bushman, Genome-wide analysis of chromosomal features repressing human immunodeficiency virus transcription. *J. Virol.* **79**, 6610–6619 (2005).  
[Medline doi:10.1128/JVI.79.11.6610-6619.2005](#)
35. L. Holmfeldt, L. Wei, E. Diaz-Flores, M. Walsh, J. Zhang, L. Ding, D. Payne-Turner, M. Churchman, A. Andersson, S. C. Chen, K. McCastlain, J. Becksfort, J. Ma, G. Wu, S. N. Patel, S. L. Heatley, L. A. Phillips, G. Song, J. Easton, M. Parker, X. Chen, M. Rusch, K. Boggs, B. Vadodaria, E. Hedlund, C. Drenberg, S. Baker, D. Pei, C. Cheng, R. Huether, C. Lu, R. S. Fulton, L. L. Fulton, Y. Tabib, D. J. Dooling, K. Ochoa, M. Minden, I. D. Lewis, L. B. To, P. Marlton, A. W. Roberts, G. Raca, W. Stock, G. Neale, H. G. Drexler, R. A. Dickins, D. W. Ellison, S. A. Shurtliff, C. H. Pui, R. C. Ribeiro, M. Devidas, A. J. Carroll, N. A. Heerema, B. Wood, M. J. Borowitz, J. M. Gastier-Foster, S. C. Raimondi, E. R. Mardis, R. K. Wilson, J. R. Downing, S. P. Hunger, M. L. Loh, C. G. Mullighan, The genomic landscape of hypodiploid acute lymphoblastic leukemia. *Nat. Genet.* **45**, 242–252 (2013). [Medline doi:10.1038/ng.2532](#)
36. I. Bozic, T. Antal, H. Ohtsuki, H. Carter, D. Kim, S. Chen, R. Karchin, K. W. Kinzler, B. Vogelstein, M. A. Nowak, Accumulation of driver and passenger mutations during tumor progression. *Proc. Natl. Acad. Sci. U.S.A.* **107**, 18545–18550 (2010). [Medline doi:10.1073/pnas.1010978107](#)
37. L. Josefsson, S. Palmer, N. R. Faria, P. Lemey, J. Casazza, D. Ambrozak, M. Kearney, W. Shao, S. Kottilil, M. Sneller, J. Mellors, J. M. Coffin, F. Maldarelli, Single cell analysis of lymph node tissue from HIV-1 infected patients reveals that the majority of CD4<sup>+</sup> T-cells contain one HIV-1 DNA molecule. *PLOS Pathog.* **9**, e1003432 (2013). 10.1371/journal.ppat.1003432 [Medline doi:10.1371/journal.ppat.1003432](#)
38. J. A. Anderson, N. M. Archin, W. Ince, D. Parker, A. Wiegand, J. M. Coffin, J. Kuruc, J. Eron, R. Swanstrom, D. M. Margolis, Clonal sequences recovered from plasma from patients with residual HIV-1 viremia and on intensified antiretroviral therapy are identical to replicating viral RNAs recovered from circulating resting CD4+ T cells. *J. Virol.* **85**, 5220–5223 (2011). [Medline doi:10.1128/JVI.00284-11](#)
39. H. P. Mok, S. Javed, A. Lever, Stable gene expression occurs from a minority of integrated HIV-1-based vectors: Transcriptional silencing is present in the majority. *Gene Ther.* **14**, 741–751 (2007). [Medline doi:10.1038/sj.gt.3302923](#)
40. K. Imai, H. Togami, T. Okamoto, Involvement of histone H3 lysine 9 (H3K9) methyltransferase G9a in the maintenance of HIV-1 latency and its reactivation by BIX01294. *J. Biol. Chem.* **285**, 16538–16545 (2010). [Medline doi:10.1074/jbc.M110.103531](#)

41. J. Friedman, W. K. Cho, C. K. Chu, K. S. Keedy, N. M. Archin, D. M. Margolis, J. Karn, Epigenetic silencing of HIV-1 by the histone H3 lysine 27 methyltransferase enhancer of Zeste 2. *J. Virol.* **85**, 9078–9089 (2011). [Medline doi:10.1128/JVI.00836-11](#)
42. P. G. Eipers, J. F. Salazar-Gonzalez, C. D. Morrow, HIV gene expression from intact proviruses positioned in bacterial artificial chromosomes at integration sites previously identified in latently infected T cells. *Virology* **410**, 151–160 (2011). [Medline doi:10.1016/j.virol.2010.11.001](#)
43. S. Sherrill-Mix, M. K. Lewinski, M. Famiglietti, A. Bosque, N. Malani, K. E. Ocwieja, C. C. Berry, D. Looney, L. Shan, L. M. Agosto, M. J. Pace, R. F. Siliciano, U. O'Doherty, J. Guatelli, V. Planelles, F. D. Bushman, HIV latency and integration site placement in five cell-based models. *Retrovirology* **10**, 90 (2013). [Medline doi:10.1186/1742-4690-10-90](#)
44. L. M. Frenkel, Y. Wang, G. H. Learn, J. L. McKernan, G. M. Ellis, K. M. Mohan, S. E. Holte, S. M. De Vange, D. M. Pawluk, A. J. Melvin, P. F. Lewis, L. M. Heath, I. A. Beck, M. Mahalanabis, W. E. Naugler, N. H. Tobin, J. I. Mullins, Multiple viral genetic analyses detect low-level human immunodeficiency virus type 1 replication during effective highly active antiretroviral therapy. *J. Virol.* **77**, 5721–5730 (2003). [Medline doi:10.1128/JVI.77.10.5721-5730.2003](#)
45. P. Armitage, Tests for linear trends in proportions and frequencies. *Biometrics* **11**, 375–386 (1955). [doi:10.2307/3001775](#)
46. K. A. Clouse, D. Powell, I. Washington, G. Poli, K. Strelbel, W. Farrar, P. Barstad, J. Kovacs, A. S. Fauci, T. M. Folks, Monokine regulation of human immunodeficiency virus-1 expression in a chronically infected human T cell clone. *J. Immunol.* **142**, 431–438 (1989). [Medline](#)
47. T. M. Folks, K. A. Clouse, J. Justement, A. Rabson, E. Duh, J. H. Kehrl, A. S. Fauci, Tumor necrosis factor alpha induces expression of human immunodeficiency virus in a chronically infected T-cell clone. *Proc. Natl. Acad. Sci. U.S.A.* **86**, 2365–2368 (1989). [Medline doi:10.1073/pnas.86.7.2365](#)
48. M. D. Daniel *et al.*, Simian immunodeficiency virus from African green monkeys. *J. Virol.* **62**, 4123–4128 (1988). [Medline](#)
49. R. Kikukawa, Y. Koyanagi, S. Harada, N. Kobayashi, M. Hatanaka, N. Yamamoto, Differential susceptibility to the acquired immunodeficiency syndrome retrovirus in cloned cells of human leukemic T-cell line Molt-4. *J. Virol.* **57**, 1159–1162 (1986). [Medline](#)
50. A. G. Rodrigo, P. C. Goracke, K. Rowhanian, J. I. Mullins, Quantitation of target molecules from polymerase chain reaction-based limiting dilution assays. *AIDS Res. Hum. Retroviruses* **13**, 737–742 (1997). [Medline doi:10.1089/aid.1997.13.737](#)
51. J. Ye, G. Coulouris, I. Zaretskaya, I. Cutcutache, S. Rozen, T. L. Madden, Primer-BLAST: A tool to design target-specific primers for polymerase chain reaction. *BMC Bioinformatics* **13**, 134 (2012). [10.1186/1471-2105-13-134](#) [Medline doi:10.1186/1471-2105-13-134](#)
52. S. L. Liu, T. Schacker, L. Musey, D. Shriner, M. J. McElrath, L. Corey, J. I. Mullins, Divergent patterns of progression to AIDS after infection from the same source: Human

immunodeficiency virus type 1 evolution and antiviral responses. *J. Virol.* **71**, 4284–4295 (1997). [Medline](#)

53. M. Altfeld, M. M. Addo, R. Shankarappa, P. K. Lee, T. M. Allen, X. G. Yu, A. Rathod, J. Harlow, K. O'Sullivan, M. N. Johnston, P. J. Goulder, J. I. Mullins, E. S. Rosenberg, C. Brander, B. Korber, B. D. Walker, Enhanced detection of human immunodeficiency virus type 1-specific T-cell responses to highly variable regions by using peptides based on autologous virus sequences. *J. Virol.* **77**, 7330–7340 (2003). [Medline](#)  
[doi:10.1128/JVI.77.13.7330-7340.2003](https://doi.org/10.1128/JVI.77.13.7330-7340.2003)
54. B. Langmead, S. L. Salzberg, Fast gapped-read alignment with Bowtie 2. *Nat. Methods* **9**, 357–359 (2012). [Medline](#) [doi:10.1038/nmeth.1923](https://doi.org/10.1038/nmeth.1923)
55. W. J. Kent, BLAT: The BLAST-like alignment tool. *Genome Res.* **12**, 656–664 (2002).  
[Medline](#) [doi:10.1101/gr.229202](https://doi.org/10.1101/gr.229202)
56. K. D. Pruitt, T. Tatusova, D. R. Maglott, NCBI Reference Sequence project: Update and current status. *Nucleic Acids Res.* **31**, 34–37 (2003). [Medline](#) [doi:10.1093/nar/gkg111](https://doi.org/10.1093/nar/gkg111)
57. F. Hsu, W. J. Kent, H. Clawson, R. M. Kuhn, M. Diekhans, D. Haussler, The UCSC Known Genes. *Bioinformatics* **22**, 1036–1046 (2006). [Medline](#) [doi:10.1093/bioinformatics/btl048](https://doi.org/10.1093/bioinformatics/btl048)
58. A. Alexa, J. Rahnenführer, T. Lengauer, Improved scoring of functional groups from gene expression data by decorrelating GO graph structure. *Bioinformatics* **22**, 1600–1607 (2006). [Medline](#) [doi:10.1093/bioinformatics/btl140](https://doi.org/10.1093/bioinformatics/btl140)
59. S. Holm, A simple sequentially rejective multiple test procedure. *Scand. J. Stat.* **6**, 65–70 (1979).